

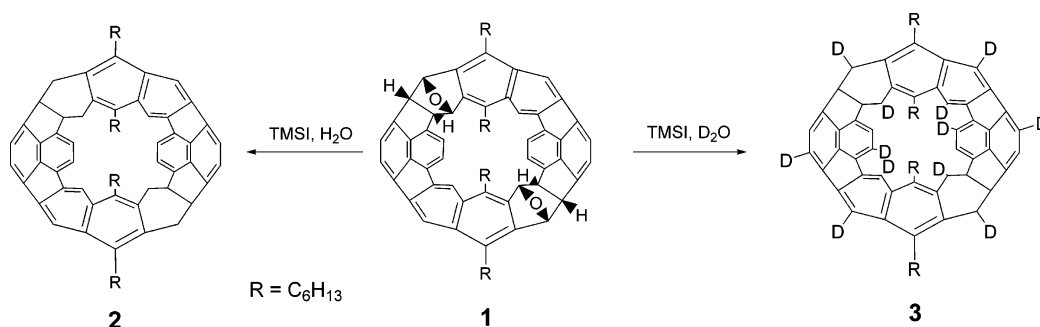
Double-Stranded Cycles: Toward C₈₄'s Belt Region

Mihaiela Stuparu,[†] Volker Gramlich,[†] Amnon Stanger,^{*,‡} and A. Dieter Schlüter^{*†}

Institute of Polymers, Department of Materials, ETH-Zürich, Wolfgang Pauli Strasse 10, HCI J 541, CH-8093 Zürich, Switzerland, and Schulich Faculty of Chemistry and The Lise-Meitner-Minerva Center for Computational Quantum Chemistry, Technion, Technion City, 32000 Haifa, Israel

dieter.schluefer@mat.ethz.ch

Received August 17, 2006

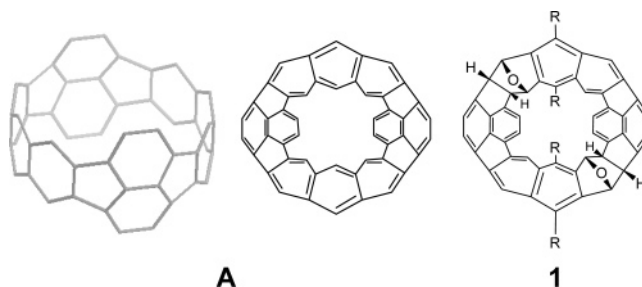


The reactivity of the double-stranded hydrocarbon cycle with two ether bridges (**1**) toward iodotrimethylsilane (TMSI) was investigated in some detail. The carbon skeleton of cycle **1** resembles the belt region of a C₈₄ fullerene which makes it a potential precursor to the long sought after fully aromatic derivative. Upon exposure to TMSI, cycle **1** undergoes a cascade of reactions which involve different states of iodination/reduction which ultimately lead to the hydrogenated cycle **5a**, whose structure was proven by single-crystal X-ray analysis. A deeper insight into mechanistic aspects of this sequence of conversions was gained by performing the reaction under dry and wet conditions, whereby the latter involved both normal and deuterated water. With the help of detailed NMR correlation studies and DFT computations, all important aspects were clarified including an unexpected selective H/D exchange at the naphthalenic moieties.

Introduction

In a long-term project aiming at the synthesis of the fully aromatic double-stranded cycle **A**, we have recently reported on the significantly improved access to compound **1**,^{1,2} which is considered either a direct precursor for **A** or a key intermediate on the way to it (Chart 1). Compound **1** can now be synthesized on a 3 g scale which enables systematic exploration of its chemistry and, thus, evaluation of its potential for direct aromatization as well as for accessing derivatives which could act as alternative precursors for **A**. In a first collection of experiments, mostly employing Brønsted and Lewis acids, it was found that compound **1** is unexpectedly stable. In contrast to noncyclic model compounds, it cannot easily be aromatized by acidic dehydration. Also, when successfully converted into certain derivatives, those when under hydrolytic conditions have

CHART 1. Spatial (Double Bonds Omitted) and Chemical Structure of the Aromatic Belt **A** and the Chemical Structure of Starting Material **1**



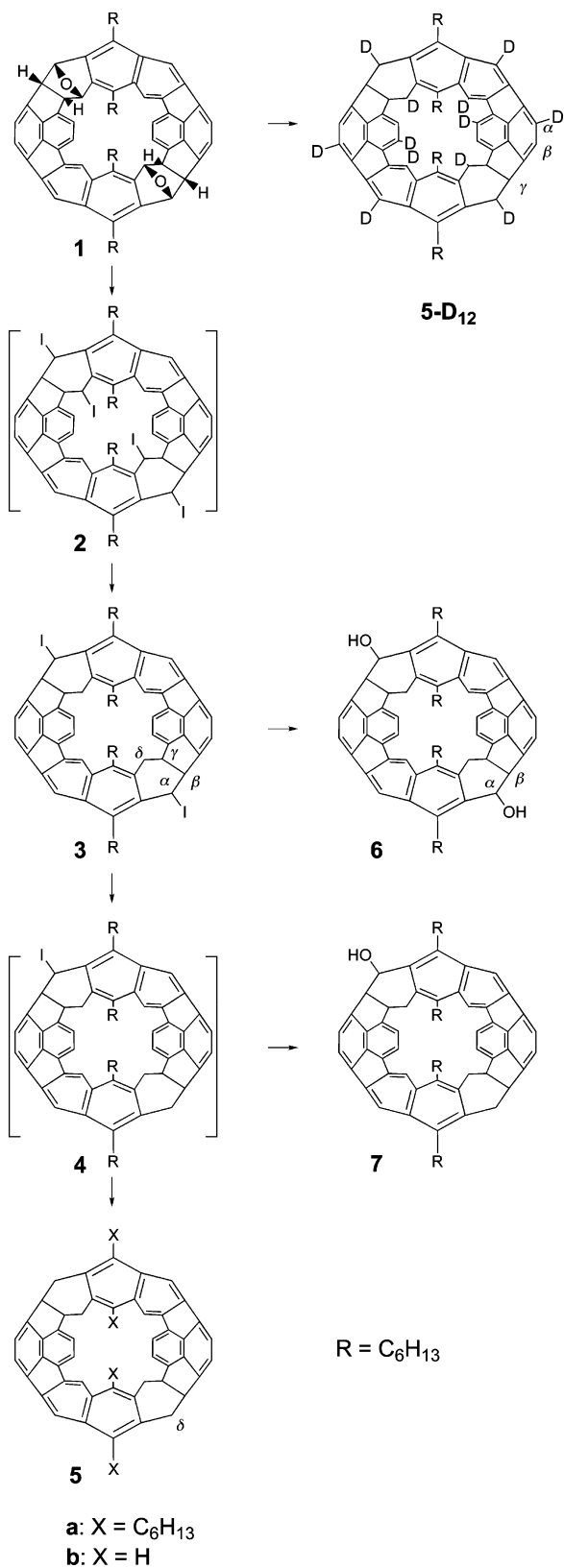
a high tendency to rebuild compound **1**. Through these investigations it became clear that the carbon skeleton of **1** avoids aromatization. In the corresponding publication,¹ the reactions of compound **1** with iodotrimethylsilane, a very potent electrophilic reagent which has found widespread applications,³ were not included. It became clear that these reactions are complex and rather represent a separate chapter in the exciting chemistry of **1**. The present work now is devoted to this very

[†] ETH-Zürich.

[‡] Technion.

(1) (a) Stuparu, M.; Lentz, D.; Rügger, H.; Schlüter, A. D. *Eur. J. Org. Chem.* **2006**, in press. (b) For the original work, see: Neudorff, W. D.; Lentz, D.; Anbarro, M.; Schlüter, A. D. *Chem. Eur. J.* **2003**, *9* (12), 2745–2757.

SCHEME 1. Suggested Mechanism for the TMSI-Induced Conversion of 1 into 5a in the Presence of Traces of Water and Deuterated Water, Respectively



aspect. It also contains a theoretical treatment of a specific reaction steps so as to provide a better understanding for the selectivity encountered.

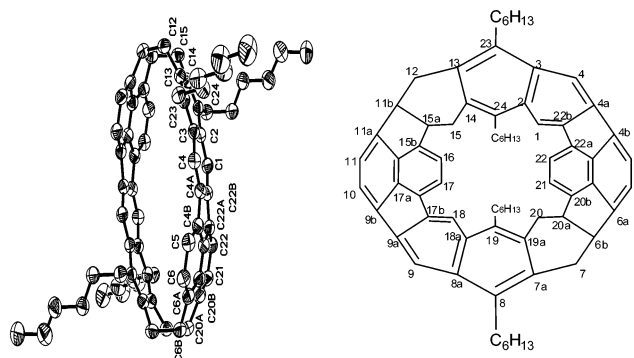


FIGURE 1. ORTEP plot of compound **5a** in the single crystal (left) with the numbering system (right). A molecule of dichloromethane contained in the unit cell is omitted.

Results and Discussion

Upon addition of approximately 4 equiv of commercially available iodotrimethylsilane (TMSI) per oxygen bridge to a solution of 50 mg of compound **1** in solvents like benzene, chloroform, and dichloromethane (DCM) at room temperature, product **5a** was reproducibly obtained in yields of 80–90% (Scheme 1). These reactions were performed in nondried solvents under air.

Compound **5a** was fully characterized (see the Supporting Information) including a single-crystal X-ray analysis (Figure 1). The structure of **5a** will be briefly discussed below. If the reaction was carried out in dry media a yellowish precipitate formed which, because of its low solubility, could not be properly characterized by NMR spectroscopy. After filtration and washing with ethanol, its exposure to wet solvents led to formation of starting material **1** almost quantitatively. In agreement with the literature in which conversions of dialkyl ethers into two iodoalkanes are described,³ it is proposed that the precipitate is the corresponding tetraiodide **2**.⁴ Follow-up reductions of iodides to the corresponding methylene groups are known but obviously do not take place here. They are proposed to be caused by hydroiodic acid,^{3f} which cannot form under the above dry conditions. In order to unravel the mechanism of the conversion of **1** to **5a** under conditions where

(2) For the corresponding linear polymers (ladder polymers), see: Schlüter, A. D. *Adv. Mater.* **1991**, *3* (6), 282–91. Schlüter, A. D.; Loeffler, M.; Enkelmann, V. *Nature* **1994**, *368* (6474), 831–4.

(3) (a) Ho, T.-L.; Olah, G. A. *Angew. Chem.* **1976**, *88* (24), 847. (b) Jung, M. E.; Lyster, M. A. *J. Org. Chem.* **1977**, *42* (23), 3761–4. (c) Olah, G. A.; Narang, S. C. *Tetrahedron* **1982**, *38* (15), 2225–77. For the cleavage of benzylic ethers with TMSI or similar reagents and the reduction of the initial products under the reaction conditions, see, for example: (d) Olah, G. A.; Narang, S. C.; Gupta, B. G. B.; Malhotra, R. *J. Org. Chem.* **1979**, *44* (8), 1247–51. (e) Sakai, T.; Miyata, K.; Utaka, M.; Takeda, A. *Tetrahedron Lett.* **1987**, *28* (33), 3817–18. (f) Stoner, E. J.; Cothron, D. A.; Balmer, M. K.; Roden, B. A. *Tetrahedron* **1995**, *51* (41), 11043–62. (g) Cain, G. A.; Holler, E. R. *Chem. Commun.* **2001**, (13), 1168–1169.

(4) We believe that compound **2** is the tetraiodo and not, e.g., the tetra-(trimethylsilyloxy) derivative because published mechanisms of how ethers and alcohols are being reduced to the corresponding alkanes by TMSI involve iodinated rather than trimethylsilyloxy intermediates. In addition, from our experience with the solubility of various double-stranded cyclic compounds it would be difficult to understand why the tetra(trimethylsilyloxy) derivative related to **2** should not be soluble under the conditions reported.

(5) Note that all lifetimes mentioned here strongly depended upon the actual concentration of TMSI. By increasing the latter by a factor of approximately 2 the same intermediates were formed but at lifetimes which were easily a factor of 10 shorter.

(6) The intermediacy of a triiodide is likely but can only be speculated.

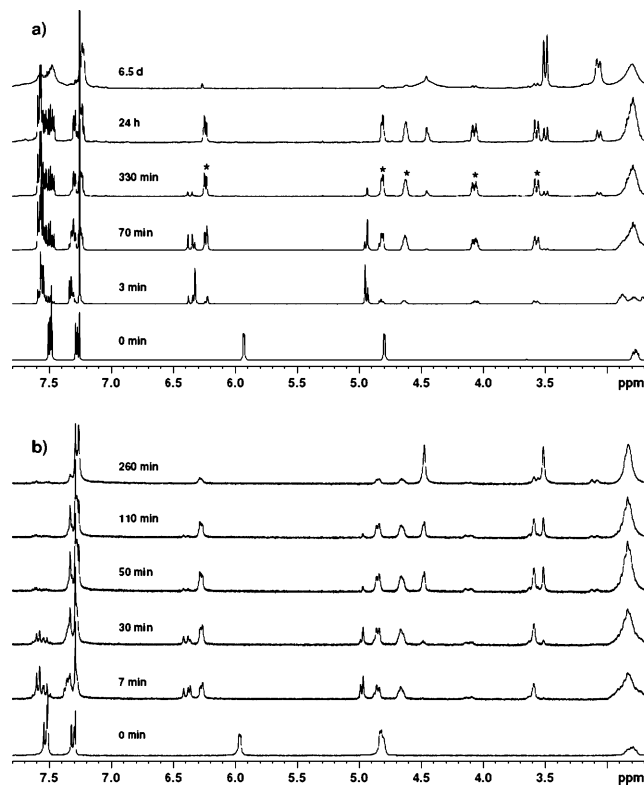


FIGURE 2. ^1H NMR spectroscopic in situ monitoring of the process by which starting material **1** is converted through several intermediates into compounds **5a** (a) and **5-D₁₂** (b), respectively, by the presence of iodotrimethylsilane (TMSI) in CDCl_3 at room temperature. Signals due to the intermediate **3** are marked with an asterisk (*).

some water is present, the reaction was monitored by in situ NMR spectroscopy. Compound **1** was dissolved in CDCl_3 (approximately 10 mg in 0.5 mL) and TMSI (1:10 = **1**/TMSI) added with an Eppendorf pipet. Immediately thereafter, NMR monitoring was started and continued for approximately 6.5 days at normal probe temperature (Figure 2a). From the very beginning there was no indication of the starting material. Instead, major new compounds were observed, the concentration of which decayed on a time scale of a few hours. The signals associated with these compounds, e.g., at $\delta = 4.90$ and 6.30 ppm, were not identified but most likely mirror the formation of the tetraiodo (**2**) and triiodo intermediates (the structure of the latter is not shown). These transient intermediates then were converted into a new one which had a lifetime in the range of a few days.⁵ Its NMR signals are marked with asterisks in the fourth trace of Figure 2a. This new intermediate was unambiguously characterized as the diiodide **3** by NMR correlation experiments (TOCSY, HMQC, HMBC; for details, see the Supporting Information). This allowed for a full assignment of the spin system expected for a moiety indicated by the assigned positions α – δ in structure **3** (Scheme 1). In addition, the chemical shifts were as expected including the most indicative high field shift of the iodinated carbon atoms denoted as α which absorbed at $\delta = 26.6$ ppm. Further and final support for the proposed intermediate **3** came from a parallel flask-type experiment in which the intermediates were continuously traced by TLC. As the spot that indicated compound **3** had maximum intensity, the reaction was quenched with either water or aqueous sodium hydrogen sulfite and compound **6** isolated on the 20 mg scale (see the Supporting Information). This compound is

the direct hydrolysis product of **3** and consists of an approximately 50:50 mixture of isomers in which the two hydroxyl groups are oriented *syn* and *anti* to one another. This quenching repeatedly but not fully reproducibly also furnished compound **7**, which is the hydrolysis product of the monoiodide **4**. After several days, finally, intermediate **3** had converted into the final product **5a**. Combining these experiments, the sequential mechanism in Scheme 1 is proposed.⁶

In the next step, the source of hydrogen in these conversions was investigated. As mentioned, if the reaction was performed in dry media it stopped at the level of compound **2**.⁴ The reaction was therefore performed in water-free solvents containing traces of deuterated water. It followed the same paths and gave compound **5-D₁₂** contaminated with some **5a**. Compound **5-D₁₂** contains 12 deuterium atoms which were selectively incorporated at the indicated positions (Scheme 1). This was proven by NMR spectral analysis. Figure 3 compares the NMR spectra of **5a** and **5-D₁₂** and also shows a long-range H,H correlation experiment. Most strikingly, the aromatic region of **5-D₁₂** shows only one singlet at $\delta = 7.27$ ppm (besides some residual **5a**). Together with the correlation experiment, which proves that the β and γ protons of **5-D₁₂** couple, this can only be explained by assuming that both of the protons of the “horizontal” naphthalenes as well as the two α H’s of the “vertical” naphthalenes were exchanged by deuterium. The δ methylene protons in **5a** absorb at $\delta = 3.10$ and 3.52 with a geminal coupling of 13 Hz. In **5-D₁₂**, the former signal disappears (except for some intensity due to residual protonated analogs) and the remaining signal at $\delta = 3.50$ appears as singlet. This is indicative of monodeuteration of each of the four δ methylene units. In addition, this monodeuteration must be selective in a sense that the deuterium atoms all either point in- or outward. The process of deuterium incorporation was also monitored over a time span of 260 min by NMR tube experiments.⁵ Typical series of spectra are shown in Figure 2b and compared with the analogous series obtained when normal water was present instead of D_2O (Figure 2a). It is evident that in the presence of deuterated water the same intermediates are formed. The comparison also allows a qualitative evaluation of the relative rates of the two different processes which take place: (a) reduction of the oxygen carrying carbon atoms of **1** to methylenes and (b) regiospecific H/D exchange of 8 of the 12 naphthalenic protons. Regarding the first aspect, it should be noted that in the intermediate **3** the intensity of one of the two protons of position δ is greatly reduced (at $\delta = 4.10$ ppm) and the respective other signal changed into a singlet (at $\delta = 3.58$ ppm). The deuteration degree is less than the expected 98%,⁷ which most likely is due to some residual normal water that could not be avoided in the experiments. Regarding the second aspect, one should notice that the significant changes in the aromatic region (Figure 2b) seem to be completed more or less once the intermediate **3** has been formed. The final conversion into **5-D₁₂** takes place thereafter. Thus, the H/D exchange is completed faster than all of the reduction steps.

The fact that not only the carbon atoms which carried the iodides but also the two different naphthalene units were deuterated supports the intermediacy of deuteriodic acid, a potent reagent for an H/D exchange according to an *ipso* electrophilic aromatic substitution (EAS) pattern. Regarding the vertical naphthalenes, it is noteworthy that it was the α and not

(7) The deuteration degree of the D_2O used was stated as 98% by the supplier.

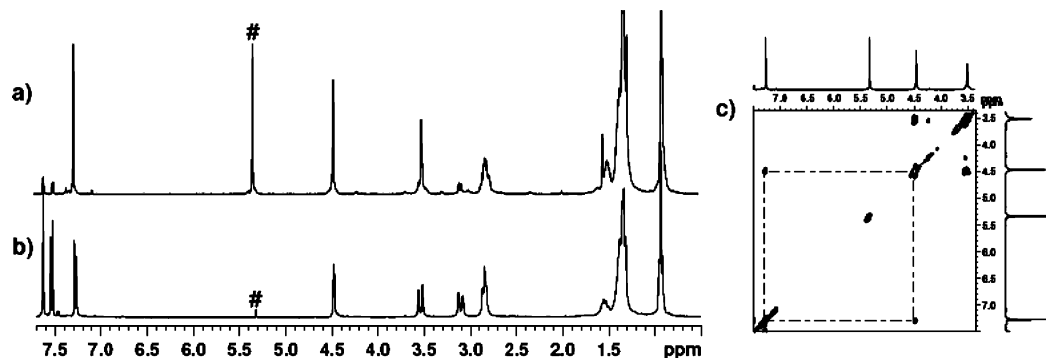


FIGURE 3. NMR spectra of compounds **5-D**₁₂ (a) and **5a** in dichloromethane (#) (b) and a part of the TOCSY correlation experiment with **5-D**₁₂ in order to prove the coupling between the positions β and γ as assigned in Scheme 1 (c).

the β positions which suffered the exchange. This is in agreement with common mechanistic considerations of EAS and also supported by NMR correlation experiments which show a coupling between the β and the γ -protons. To further substantiate this and also to exclude any eventual influence of curvature which may cause an unexpected selectivity, this aspect was also treated theoretically by using DFT computations (see the Experimental Section for the method and meaning of numbers discussed).⁸

The structure of computed **5b** (hexyl chains omitted) is in very good agreement with the experimentally determined one (**5a**). For example, the average absolute error in bond length is 0.0094 Å, the largest being 0.0257 Å. It thus seems that the theoretical level used can treat this compound properly. To address the selectivity issue, compound **5b** was protonated in α and independently in β position, and the energies of the two resulting intermediates were compared. The comparison shows that α -protonated **5b** is more stable by 3.5 (3.5) kcal mol⁻¹ than the β -protonated one, suggesting that the former will be the one obtained through EAS mechanism, where the *ipso* protonated ion (σ -complex) is the key intermediate. However, it has been shown previously that the hydroniumated (i.e., the complex between the proton and H₂O) and protonated benzene have different geometrical properties.⁹ Thus, α - and β -hydroniumated **5b** were also calculated to account for any change that this presumably more realistic binding situation may have

on the preference of protonation. It was found that the stability order did not change, although the energy difference was reduced to 1.9 (2.0) kcal mol⁻¹. In contrast to the benzene example, the structure near the protonation site did not change much by adding the water molecule. In the case of **5b** the water acts like a relatively remote solvent, with H₂O–H distances of 2.305 and 2.051 Å for the α and β hydroniumated **5b**, respectively. Thus, the computations fully support the selectivity of the α deuteration.

In order to get a better understanding of the protonation process and to gain even more confidence in the calculations some additional aspects were studied. First, the experimental and calculated proton affinities (PAs) of benzene and naphthalene were compared. They are 182.2 and 196.3 (α) [193.3 (β)] kcal mol⁻¹, respectively, whereas the experimental respective numbers are 179.3 and 191.9 (no topical information for naphthalene).¹⁰ Thus, within ~ 3 kcal mol⁻¹ B3LYP/6-311G* can be trusted for PA calculations. The theoretical level used here performs even better for PAs differences. Thus, the difference between the experimental PAs of benzene and naphthalene and that of the calculated benzene and the average PA of naphthalene is identical (12.6 kcal mol⁻¹).

The α and β PAs of **5b** are 215.6 and 212.1 kcal mol⁻¹, respectively. The main resonance structures of the α - and β -protonated **5b** suggest that the difference is that the cation in the α protonated **5b** is stabilized by two phenyl groups, whereas the β protonated **5b** is stabilized by a phenyl and an alkyl. Thus, the 3.5 kcal mol⁻¹ difference in stability seems small compared with the difference between diphenyl carbenium and methylphenyl carbenium ions, which is 12.5(12.5) kcal mol⁻¹ at the same theoretical level.¹¹ The following questions remained to be answered: (a) Is the larger PA of **5b** relative to benzene and naphthalene only a size effect, or are there other reasons? (b) Why are the differences between α - and β -protonated **5b** smaller than expected? To answer them, a fragment of **5b**, α -protonated **5b**, and β -protonated **5b** which contains the naphthalene moiety with the fused five- and six-membered ring (**5fr**, α -**H-5fr**, and β -**H-5fr**, respectively) were calculated at their geometries in **5b** (four C–C bonds replaced by four C–H bonds with standard bond lengths) and then allowed to relax geometrically (Figure 4).

(8) Gaussian 03, Revisions B.05 and C.02: Frisch, M. J.; Trucks, G. W.; Schlegel, H. B.; Scuseria, G. E.; Robb, M. A.; Cheeseman, J. R.; Montgomery, J. A., Jr.; Vreven, T.; Kudin, K. N.; Burant, J. C.; Millam, J. M.; Iyengar, S. S.; Tomasi, J.; Barone, V.; Mennucci, B.; Cossi, M.; Scalmani, G.; Rega, N.; Petersson, G. A.; Nakatsuji, H.; Hada, M.; Ehara, M.; Toyota, K.; Fukuda, R.; Hasegawa, J.; Ishida, M.; Nakajima, T.; Honda, Y.; Kitao, O.; Nakai, H.; Klene, M.; Li, X.; Knox, J. E.; Hratchian, H. P.; Cross, J. B.; Bakken, V.; Adamo, C.; Jaramillo, J.; Gomperts, R.; Stratmann, R. E.; Yazyev, O.; Austin, A. J.; Cammi, R.; Pomelli, C.; Ochterski, J. W.; Ayala, P. Y.; Morokuma, K.; Voth, G. A.; Salvador, P.; Dannenberg, J. J.; Zakrzewski, V. G.; Dapprich, S.; Daniels, A. D.; Strain, M. C.; Farkas, O.; Malick, D. K.; Rabuck, A. D.; Raghavachari, K.; Foresman, J. B.; Ortiz, J. V.; Cui, Q.; Baboul, A. G.; Clifford, S.; Cioslowski, J.; Stefanov, B. B.; Liu, G.; Liashenko, A.; Piskorz, P.; Komaromi, I.; Martin, R. L.; Fox, D. J.; Keith, T.; Al-Laham, M. A.; Peng, C. Y.; Nanayakkara, A.; Challacombe, M.; Gill, P. M. W.; Johnson, B.; Chen, W.; Wong, M. W.; Gonzalez, C.; Pople, J. A. Gaussian, Inc., Wallingford CT, 2004.

(9) The *ipso*-protonated benzene is the global minimum for the cyclic C₆H₇⁺, whereas the edge-protonated structure is a transition state ($n_{\text{imag}} = 1$) for the 1,2-shift of a proton between the two *ipso*-protonated structures. However, when a molecule of water is added to the system (hydroniumated benzene), the edge-hydroniumated structure becomes a minimum. See: (a) Kryachko, E. S.; Nguyen, M. T. *J. Phys. Chem. A* **2001**, *105* (1), 153–155. (b) Denekamp, C.; Stanger, A. *J. Mass Spectrom.* **2002**, *37* (3), 336–342.

(10) NIST Standard Reference Database No. 69, June 2005 release. See: <http://webbook.nist.gov/chemistry/>.

(11) From the hydride-transfer isodesmic reaction between the two ions and the respective neutrals.

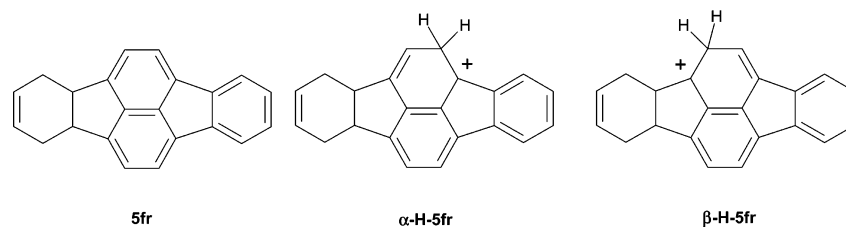


FIGURE 4. Protonated and nonprotonated fragments used for comparative model computations.

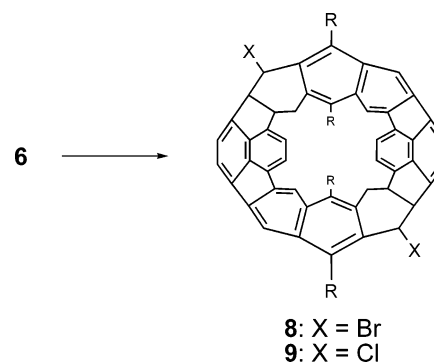
The PAs for α - and β -protonated **5fr** are 205.2 and 207.7 at their geometries in the belt and 205.5 and 208.1 in their optimized geometries.¹² Evidently, the geometry optimization did not greatly change the PAs, which are in between the PAs of naphthalene and those of **5b**. Thus, it is safe to deduce that the larger PA of **5b** relative to benzene and naphthalene is mostly a size effect. However, there is a change in stability order; β -H-**5fr** is more stable than α -H-**5fr** by 2.5 and 2.6 kcal mol⁻¹ for the nonoptimized and the optimized geometries, respectively. The reason is strain-induced bond localization (SIBL).¹³ As evident from the geometry of **5fr**, the strain induced by the annulated five-membered rings causes the naphthalenic bonds to localize, the bonds exocyclic to these rings to get shorter (1.3890, 1.3704, and 1.3869 Å) and the endocyclic bonds to become longer (1.4356, 1.4058, and 1.3991 Å). On β protonation this localization can persist, but in α protonation it is inverted, causing an increased amount of strain to be built in the latter, and become less stable despite the electronic effect. In **5b**, the excess strain is released through the macrocycle, causing the electronic effect to dominate, although the difference between the two isomers is much less than expected according to pure electronic reasons (see above). For example, the average change in bond length of the β -six-membered ring (i.e., the ring which is not included in the models **5-fr**) between α protonated **5b** and **5b** is 0.073 Å, but the same respective difference between β protonated **5b** and **5b** is only 0.0010 Å. Thus, the observed preference for protonation of **5a** in the α position is the result of contradicting electronic and strain effects. In the macrocycle, where the strain can be distributed over the whole

(12) The values reported in the text for PAs are the standard enthalpy for the protonation reaction. Since **5fr** and its protonation products at their geometry in **5b** are nonoptimized structures their calculated thermodynamic parameters are questionable. The PAs from total energies of the nonstructurally optimized species are 212.4 and 214.9 kcal mol⁻¹ for α -H-**5fr** and β -H-**5fr**, respectively, whereas for the optimized structures the PAs for the total energies are 212.8 and 215.4, respectively. Thus, the difference in PAs between α -H-**5fr** and β -H-**5fr** resulting from the total energies of the nongeometrically optimized structures is identical to that obtained from the enthalpy differences (2.5 kcal mol⁻¹) and very similar to that obtained from the total energies and enthalpies of the optimized structures (2.6 kcal mol⁻¹).

(13) (a) Stanger, A. *J. Am. Chem. Soc.* **1991**, *113* (22), 8277–80. (b) Stanger, A.; Boese, R.; Askenazi, N.; Stellberg, P. *J. Organomet. Chem.* **1997**, *542* (1), 19–24. (c) Stanger, A.; Boese, R.; Askenazi, N.; Stellberg, P. *J. Organomet. Chem.* **1997**, *548* (1), 113. (d) Stanger, A.; Boese, R.; Ashkenazi, N.; Stellberg, P. *J. Organomet. Chem.* **1998**, *556* (1–2), 249–250. (e) Stanger, A. *J. Am. Chem. Soc.* **1998**, *120* (46), 12034–12040. (f) Stanger, A.; Tkachenko, E. *J. Comput. Chem.* **2001**, *22* (13), 1377–1386. (g) Rosenau, T.; Ebner, G.; Stanger, A.; Perl, S.; Nuri, L. *Chem. Eur. J.* **2005**, *11* (1), 280–287.

(14) For some publications in which a DCTB matrix was used, see: (a) Siedschlag, C.; Luftmann, H.; Wolff, C.; Mattay, J. *Tetrahedron* **1997**, *53* (10), 3587–3592. (b) Rucareanu, S.; Mongin, O.; Schuwey, A.; Hoyler, N.; Gossauer, A.; Amrein, W.; Hediger, H.-U. *J. Org. Chem.* **2001**, *66* (15), 4973–4988. (c) Daniel, J. M.; Ehala, S.; Friess, S. D.; Zenobi, R. *Analyst* **2004**, *129* (7), 574–578. (d) Felder, T.; Schalley, C. A.; Fakhrabavi, H.; Lukin, O. *Chem. Eur. J.* **2005**, *11* (19), 5625–5636.

SCHEME 2. Conversion of the Dihydroxide **6** (Mixture of *Syn* and *Anti* Isomers) into the Corresponding Dibromide (**8**) and Dichloride (**9**)



system the electronic effect dominates. However, when only the unit that undergoes protonation is considered (**5fr**) strain dominates.

There are two final points which still need to be addressed. First, it was tried whether the hydroxyl groups in **6** could be replaced by halogen atoms in order to test whether starting materials for base-induced eliminations could be made available this way (Scheme 2). For that purpose, in an NMR tube experiment a chloroform solution of compound **6** was treated with either phosphorus tribromide or hydrochloric acid which led to clean transformations into **8** and **9**, respectively. The structures of **8** and **9** were proven by NMR spectroscopy and mass spectrometry. Upon aqueous workup both hydrolyzed to the starting material **6**, which is another support for the proposed structures.

Second, there are a few aspects of the single-crystal X-ray structure of **5a** worth being mentioned. As expected, compound **5a** has an ellipsoidal shape (Figure 1) with the longest diameter of 11.75(2) Å found between C6–C6a and the shortest one of 4.80(1) Å between C2–C2a. The angle between the rings condensed to one another via C2–C3 is 10.4(1)°, and the lines C6a–C6b and C20a–C20b deviate by 14.5(1)° from the corresponding six ring planes. For the lines C4b–C4a and C22a–C22b, the corresponding deviation amounts to 12.0(1)°.

Experimental Section

Theoretical Methods. Gaussian 03⁸ was used for the calculations. All of the molecules and ions underwent full optimization at the B3LYP/6-311G* theoretical level, and analytical frequency calculations were carried out to ensure real minima (number of imaginary frequencies – $n_{\text{imag}} = 0$) and to obtain the zero-point-energy (ZPE) and thermodynamic parameters. Reported are ZPE-corrected total energies and ΔH (in parentheses) in kcal mol⁻¹. The $\Delta H_{\text{T}}^{\circ}$ of the respective protonation reactions are reported for proton affinities (PAs).

Crystal Structure. Crystals of **5a** for X-ray structure analysis were obtained by slow evaporation of the solvent from a methylene

chloride solution. A crystal (0.2 × 0.2 × 0.1 mm) was mounted on top of a glass fiber and measured with a CAD4 diffractometer Cu K α radiation ($\lambda = 1.54178 \text{ \AA}$) with a graphite monochromator. Monoclinic, space group $P2_1/n$, $a = 12.907(3) \text{ \AA}$, $b = 17.163(3) \text{ \AA}$, $c = 13.244(5) \text{ \AA}$, $\beta = 106.09(3)^\circ$, $V = 2818.9(10) \text{ \AA}^3$, $Z = 2$, $\theta_{\text{max}} = 65.94^\circ$, 5151 measured, 4920 independent reflections, $R(\text{int}) = 0.031$, 3102 observed with $I \geq 2\sigma(I)$. The structure was solved by direct methods and refined by full-matrix least-squares in full matrix against F^2 , non-H atoms anisotropic with the standard SHELX software. The hydrogen atoms were included with geometrically calculated positions and refined using "riding model". 354 parameters, $R_1 = 0.061$, $wR_2 = 0.1905$, GOF = 1.067. The highest residual electron density is 0.32 e \AA^{-3} .

Crystallographic data (excluding structure factors) for the structure reported in this paper have been deposited with the Cambridge Crystallographic Data Centre as supplementary publication number CCDC-613926. Copies of the data can be obtained free of charge on application to CCDC, 12 Union Road, Cambridge CB2 1EZ, UK (Fax: (+44)1223-336-033; e-mail: deposit@ccdc.cam.ac.uk).

8,19,23,24-Tetrahexyl-1,1,4,4,4a,9,9,9a,17b,18,18,22b-dodecahydro-2,14:3,13-dimethenodiindeno[1,2,3-*c,d*:1',2',3'-*c',d'*]benzo[2,3-*j*:5,6-*j'*]difluoranthene (5a). To a solution of compound **1** (50 mg, 0.05 mmol) in dichloromethane (15 mL) at rt was added trimethylsilyl iodide (152 μL , 1.07 mmol) at once, and the reaction mixture was allowed to stir at rt. The reaction course was followed using TLC (hexane/dichloromethane 1:1). Upon addition of the trimethylsilyl iodide, the color changed slowly to brown. After the conversion into compound **5** was completed, the reaction was quenched using aq NaHSO₃. Stirring was continued until the solution had turned yellow. The organic phase was dried over MgSO₄ and the solvent removed under reduce pressure. Compound **5** was purified using column chromatography on silica gel eluting with a mixture of hexane/ dichloromethane 1:1 ($R_f = 0.9$) to give a yellow solid (40 mg, 88%). Single crystals of **5** for X-ray diffraction were obtained by slow evaporation of the solvent of a solution of **5** in dichloromethane. ¹H NMR (500 MHz, CDCl₃): δ 7.58 (s, 4 H, H-7, -12, -15, -20), 7.49 (d, ³ $J = 7.0 \text{ Hz}$, 4 H, H-6, -11, -16, -21), 7.24 (d, ³ $J = 7.0 \text{ Hz}$, 4 H, H-5, -10, -17, -22), 4.46 (s, 4 H, H-4a, -9a, -17b, -22b), 3.51 (d, ² $J = 13.4 \text{ Hz}$, 4 H, H-1, -4, -9, -18), 3.08 (d, ² $J = 13.4 \text{ Hz}$, 4 H, H-1, -4, -9, -18), 2.80 (m, 8 H, CH₂(CH₂)₄CH₃), 1.53–1.31 (m, 32 H, CH₂(CH₂)₄CH₃), 0.89 (m, 12 H, CH₂(CH₂)₄CH₃). ¹³C NMR (125 MHz, CDCl₃): δ 147.95, 138.44, 135.95, 134.08, 133.94, 133.38, 132.39, 129.72, 121.25, 120.23, 115.77, 46.40, 31.81, 31.40, 30.67, 29.68, 29.52, 28.17, 22.68, 13.88. HR MALDI MS: C₇₂H₇₆ calcd 940.5947, found 940.5942 [M]⁺.

8,19,23,24-Tetrahexyl-1,4,6,7,9,11,12,15,16,18,20,21-dodeca-deutero-1,4,4a,9,9a,17b,18,22b-octahydro-2,14:3,13-dimethenodiindeno[1,2,3-*c,d*:1',2',3'-*c',d'*]benzo[2,3-*j*:5,6-*j'*]difluoranthene (5-D₁₂). A solution of **1** (10 mg, 0.01 mmol) in dry CDCl₃ (0.5 mL) was prepared in a NMR tube and a small drop of D₂O added. Then trimethylsilyl iodide (14 μL , 0.10 mmol) was added at once. Upon this addition the color slowly changed to brown. The transformation of **1** into **5-D₁₂** was followed by NMR spectroscopy which showed that the reaction was complete within 5 h (see main text). The solvent was removed under reduced pressure conditions, and compound **5-D₁₂** was purified using column chromatography on silica gel eluting with a mixture of hexane/dichloromethane 1:1 ($R_f = 0.9$). ¹H NMR (500 MHz, CD₂Cl₂): δ 7.26 (s, 4 H, H-5, -10, -17, -22), 4.45 (s, 4 H, H-4a, -9a, -17b, -22b), 3.50 (s, 4 H, H-1, -4, -9, -18), 2.81 (m, 8 H, CH₂(CH₂)₄CH₃), 1.53–1.27 (m, 32 H, CH₂(CH₂)₄CH₃), 0.90 (m, 12 H, CH₂(CH₂)₄CH₃). HR MALDI MS: C₇₂H₆₄D₁₂ calcd 952.6700, found 952.6520 [M]⁺.

4,18-Dihydroxy-8,19,23,24-tetrahexyl-1,1,4,4a,9,9,9a,17b,18,22b-decahydro-2,14:3,13-dimethenodiindeno[1,2,3-*c,d*:1',2',3'-*c',d'*]benzo[2,3-*j*:5,6-*j'*]difluoranthene (C₁) + 4,9-dihydroxy-8,19,23,24-tetrahexyl-1,1,4,4a,9,9a,17b,18,18,22b-decahydro-2,14:3,13-dimethenodiindeno[1,2,3-*c,d*:1',2',3'-*c',d'*]benzo[2,3-*j*:5,6-*j'*]difluoranthene (C₂) (6). To a solution of compound **1** (100 mg, 0.103 mmol) in dichloromethane (15 mL) at rt was added trimethylsilyl iodide (176 μL , 1.2 mmol) at once, and the reaction mixture was stirred at rt. Upon this addition the color changed slowly to brown. The reaction course was followed by TLC (hexane/dichloromethane 1:3), whereby compounds **1**, **6**, **7**, and **5** eluted at the following R_f values: 0.49, 0.25, 0.6, and 0.9, respectively. As soon as compound **5** started to form (approximately 2 h), the reaction was quenched with aq NaHSO₃. The two phases were separated, and the organic phase was washed once with water (10 mL). After the phase was dried over MgSO₄, the solvent was removed under reduced pressure. The residue was purified using column chromatography on silica gel (hexane/ dichloromethane 1:2) to give compound **6** ($R_f = 0.25$) as a yellow powder (60 mg, 60%). ¹H NMR (500 MHz, CD₂Cl₂): δ 7.62, 7.61, 7.62 (3 s, 4 H, H-7, -12, -15, -20), 7.57–7.47 (overlapping signals, 4 H, H-5, -10, -17, -22), 7.33–7.27 (overlapping signals, 4 H, H-6, -11, -16, -21), 5.73 (2 d, ³ $J = 2.5 \text{ Hz}$, ³ $J = 2.4 \text{ Hz}$, 2 H, C₁: H-1, -9; C₂: H-4, -9), 4.55 (m, 4 H, H-1b, -4a, -9a, -18b), 3.99 (dd, ² $J = 13.4 \text{ Hz}$, ³ $J = 4.3 \text{ Hz}$, 2 H, C₁: H-4, -18; C₂: H-1, -18), 3.42 (2 dd, ² $J = 13.4 \text{ Hz}$, ³ $J = 2.3 \text{ Hz}$, 2 H, C₁: H-4, -18; C₂: H-1, -18), 2.94–2.74 (m, 8 H, CH₂(CH₂)₄CH₃), 2.24, 2.23 (2s, 2 H, OH), 1.60–1.27 (m, 32 H, CH₂(CH₂)₄CH₃), 0.89 (m, 12 H, CH₂(CH₂)₄CH₃). ¹³C NMR (125 MHz, CD₂Cl₂): δ 148.32, 138.1, 138.02, 134.84, 134.62, 134.40, 134.10, 132.20, 129.89, 129.72, 121.55, 121.34, 120.89, 120.75, 120.49, 120.35, 116.54, 116.40, 116.00, 115.84, 72.62, 53.62, 45.47, 32.15, 31.90, 31.87, 31.36, 30.07, 30.03, 29.99, 29.80, 29.64, 28.01, 27.99, 27.97, 27.94, 22.78, 13.98. HR MALDI MS: C₇₂H₇₆O₂ calcd 972.5840, found 972.55859 [M]⁺.

1-Hydroxy-8,19,23,24-tetrahexyl-1,4,4a,9,9,9a,17b,18,18,22b-undecahydro-2,14:3,13-dimethenodiindeno[1,2,3-*c,d*:1',2',3'-*c',d'*]benzo[2,3-*j*:5,6-*j'*]difluoranthene (7). The procedure was as described for compound **6**. The R_f value of **7** was 0.6, which allowed this compound's separation from the rest. Yield of **7** as a yellow powder: 18 mg, 19%. ¹H NMR (500 MHz, CD₂Cl₂): δ 7.63, 7.62, 7.61, 7.60 (s, 4 H, H-7, -12, -15, -20), 7.54–7.47 (overlapping signals, 4 H, H-5, -10, -17, -22), 7.33–7.26 (overlapping signals, 4 H, H-6, -11, -16, -21), 5.72 (s, 1 H, H-1), 4.53 (s, 2 H, H-1b, -4a), 4.47 (s, 2 H, H-9a, -18b), 3.99 (dd, ² $J = 13.6 \text{ Hz}$, ³ $J = 4.0 \text{ Hz}$, 1 H, H-4), 3.52 (d, ² $J = 13.3 \text{ Hz}$, 2 H, H-9, -18), 3.42 (d, ² $J = 13.3 \text{ Hz}$, 1 H, H-4), 3.08 (d, ² $J = 13.5 \text{ Hz}$, 2 H, H-9, -18), 2.92–2.79 (m, 8 H, CH₂(CH₂)₄CH₃), 2.25 (s, 1 H, OH), 1.58–1.31 (m, 32 H, CH₂(CH₂)₄CH₃), 0.90 (m, 12 H, CH₂(CH₂)₄CH₃). ¹³C NMR (125 MHz, CD₂Cl₂): δ 148.32, 148.29, 148.13, 145.40, 138.57, 138.12, 136.95, 136.24, 136.05, 135.97, 134.80, 134.67, 134.58, 134.44, 134.39, 134.24, 133.83, 133.58, 133.57, 132.58, 132.43, 132.19, 131.14, 130.02, 129.87, 129.73, 121.56, 121.42, 121.34, 120.69, 120.60, 120.54, 120.21, 116.37, 116.12, 115.97, 115.83, 72.68, 46.55, 45.48, 32.19, 31.96, 31.93, 31.91, 31.53, 31.40, 30.79, 30.72, 30.11, 29.83, 29.68, 29.66, 28.28, 28.04, 27.99, 22.85, 22.83, 22.81, 22.78, 14.03. HR MALDI MS: C₇₂H₇₆O₁ calcd 956.5891, found 956.5891 [M]⁺.

4,18-Dibromo-8,19,23,24-tetrahexyl-1,1,4,4a,9,9,9a,17b,18,22b-decahydro-2,14:3,13-dimethenodiindeno[1,2,3-*c,d*:1',2',3'-*c',d'*]benzo[2,3-*j*:5,6-*j'*]difluoranthene (C₁) + 4,9-Dibromo-8,19,23,24-tetrahexyl-1,1,4,4a,9,9a,17b,18,18,22b-decahydro-2,14:3,13-dimethenodiindeno[1,2,3-*c,d*:1',2',3'-*c',d'*]benzo[2,3-*j*:5,6-*j'*]difluoranthene (C₂) (8). A solution of **6** (5 mg) in CDCl₃ (0.5 mL) was prepared in an NMR tube, and a drop of PBr₃ was added. The reaction was monitored using ¹H NMR spectroscopy. The conversion into compound **8** was completed within 30 min. Attempts to isolate compound **8** using aqueous conditions provided only the starting compound **6**. The spectral data listed below therefore stem from the raw compound. ¹H NMR (300 MHz, CDCl₃): δ 7.62–7.27 (overlapping signals, 12 H), 6.08 (s, C₁: H-1, -9; C₂: H-4, -9), 4.82 (d, ³ $J = 6.4 \text{ Hz}$, 2 H, C₁: H-4a, -18b; C₂: H-1b, -18b), 4.65 (s, 2 H, C₁: H-1b, -9a; C₂: H-4a, -9a), 4.17 (dd, ² $J = 14.1 \text{ Hz}$, ³ $J = 5.1 \text{ Hz}$, 2 H, C₁: H-4, -18; C₂: H-1, -18), 3.53 (d, ² $J = 14.5 \text{ Hz}$, 2 H, C₁: H-4, -18; C₂: H-1, -18), 2.84 (m, 8 H,

$\text{CH}_2(\text{CH}_2)_4\text{CH}_3$), 1.55–1.15 (m, 32 H, $\text{CH}_2(\text{CH}_2)_4\text{CH}_3$), 0.91 (m, 12 H, $\text{CH}_2(\text{CH}_2)_4\text{CH}_3$). ^{13}C NMR (75 MHz, CDCl_3): δ 147.60, 146.11, 137.58, 137.11, 136.35, 135.15, 135.02, 134.82, 134.18, 131.50, 131.40, 134.18, 130.05, 131.01, 129.68, 121.80, 121.47, 121.21, 121.15, 120.68, 120.63, 116.70, 116.50, 116.17, 115.96, 54.49, 49.64, 49.60, 45.38, 32.82, 32.01, 31.77, 31.10, 30.85, 29.79, 29.66, 29.65, 29.45, 28.17, 28.10, 28.01, 22.75, 22.69, 14.29. HR MALDI MS: $\text{C}_{72}\text{H}_{76}\text{Br}_2$ calcd 1096.4157, found 1096.4172 $[\text{M}]^+$.

4,18-Dichloro-8,19,23,24-tetra-hexyl-1,1,4,4a,9,9,9a,17b,18,22b-decahydro-2,14:3,13-dimethenodiindeno[1,2,3-*c,d*:1',2',3'-*c',d'*]benzo[2,3-*j*:5,6-*j'*]difluoranthene (C_1) + 1,18-Dihydro-4,9-dichloro-8,19,23,24-tetrahexyl-1,1,4,4a,9,9a,17b,18,18,22b-decahydro-2,14:3,13-dimethenodiindeno[1,2,3-*c,d*:1',2',3'-*c',d'*]benzo[2,3-*j*:5,6-*j'*]difluoranthene (C_2) (9). A solution of **6** (10 mg) in CDCl_3 (0.5 mL) was prepared in an NMR tube, and a drop of HCl was added. The transformation of **6** into **9** was followed by NMR spectroscopy, which showed that the reaction was complete within 1 h. Attempts to isolate compound **9** using aqueous treatment provided only the starting compound **6** almost quantitatively. The spectral data listed below therefore stem from the raw compound. ^1H NMR (300 MHz, CDCl_3): δ 7.63–7.29 (overlapped signals, 12 H), 5.75 (2 d, $^3J = 2.5$ Hz, 2 H, $^3J = 2.2$ Hz C_i : H-1, -9; C_2 : H-4, -9), 4.74 (m, 2 H, C_i : H-1b, -9a, C_2 : H-4a, -9a), 4.64 (m, 2 H, C_i :

H-4a, -18b, C_2 : H-1b, -18b), 4.12 (dd, $^2J = 13.6$ Hz, $^3J = 4.7$ Hz, 2 H, C_i : H-4, -18; C_2 : H-1, -18), 3.5 (d, $^2J = 13.4$ Hz, 2 H, C_i : H-4, -18; C_2 : H-1, -18), 2.84 (m, 8 H, $\text{CH}_2(\text{CH}_2)_4\text{CH}_3$), 1.61–1.31 (m, 32 H, $\text{CH}_2(\text{CH}_2)_4\text{CH}_3$), 0.9 (m, 12 H, $\text{CH}_2(\text{CH}_2)_4\text{CH}_3$). ^{13}C NMR (75 MHz, CDCl_3): δ 147.52, 145.47, 145.22, 137.67, 137.64, 137.18, 137.02, 136.26, 136.08, 135.15, 135.00, 134.99, 134.76, 134.73, 134.13, 134.10, 131.41, 131.39, 129.92, 129.89, 129.71, 129.45, 121.63, 121.25, 121.10, 120.99, 120.54, 120.45, 116.58, 116.38, 116.05, 115.85, 58.84, 54.28, 45.27, 31.70, 31.68, 31.13, 31.04, 29.54, 29.50, 28.13, 28.06, 27.98, 22.65, 22.59, 14.14, 14.10, 14.08. HR MALDI MS: $\text{C}_{72}\text{H}_{76}\text{Cl}_2$ calcd 1008.5167, found 1008.5181 $[\text{M}]^+$.

Acknowledgment. This work was supported by the Swiss National Science Foundation and is gratefully acknowledged.

Supporting Information Available: Representative NMR spectra for all compounds. Atom coordinates and absolute energies for the theoretical calculation. This material is available free of charge via the Internet at <http://pubs.acs.org>.

JO0617114